ACS APPLIED BIO MATERIALS

Article

Cite This: ACS Appl. Bio Mater. 2019, 2, 266−276

www.acsabm.org

On Demand Release and Retrieval of Bacteria from Microwell Arrays Using Photodegradable Hydrogel Membranes

André J. van der Vlies,[†] Niloy Barua,[†] Priscila A. Nieves-Otero,[‡] Thomas G. Platt,*[,‡] and Ryan R. Hansen*[,†]

[†]Chemical Engineering Department, Kansas State University, 1701A Platt Street, Manhattan, Kansas 66506, United States

[‡]Division of Biology, Kansas State University, 1717 Claflin Road, Manhattan, Kansas 66506, United States

Supporting Information

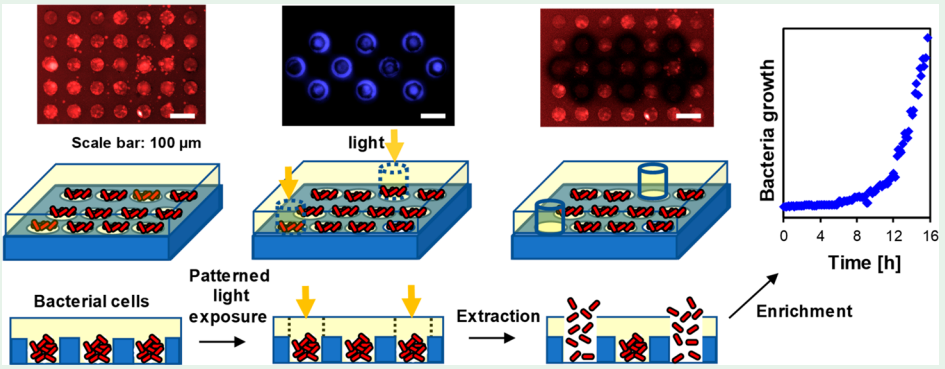

ABSTRACT: Microwell arrays are important tools for studying single cell behavior and cell−cell interactions, both in microbial and mammalian systems. However, retrieval of cells from microwell arrays with high spatial precision remains a major technical hurdle that prevents follow-up genetic and phenotypic characterization of cells within observed microwells. This work describes a new, material-based approach to grow and retrieve live bacterial cells from small (≥20 μm diameter) microwells in an array using the plant pathogen *Agrobacterium tumefaciens* as a model bacterium. Our approach uses a light-responsive, step-polymerized poly(ethylene glycol) hydrogel interface as a membrane that confines motile cells within microwells while allowing nutrient exchange and cell growth. The key design feature is the photodegradability of the membrane, as it enables individual wells of interest to be opened using patterned UV light for selective release and retrieval of cells. Extraction can occur in parallel from any number and combination of wells defined by the user. These advancements represent a new use for light-responsive hydrogels and the ability to retrieve cells from microwells with high spatial precision enables several applications that require the isolation and characterization of cells with rare phenotypes from heterogeneous populations.

KEYWORDS: *high-throughput screening, patterned illumination, microwell arrays, hydrogels, cell retrieval*

INTRODUCTION

Microwell arrays allow for high-throughput manipulation and study of cells. These platforms have several key features including their small size, high well density, and ease with which they allow for cell confinement.[1−5] In recent years, microwell arrays have been used to probe single cells to understand cellular heterogeneity[6] and rare cell function,[7] among other applications.[8,9] While the majority of microwell applications focus on mammalian systems, microwells are also useful in the study of microbial systems. These platforms have been used to examine mutant libraries[10] and to characterize the growth dynamics of single bacterial cells.[11] If microwells are large enough to confine multiple cells or designed to promote exchange of materials between wells, they become excellent tools for studying cell−cell interactions.[5,12] In this context, microwell formats have been used to examine the ecological dynamics of microbial communities under selective environmental pressures,[13,14] the consequences of contact-mediated interactions,[15] and quorum sensing.[11,16]

Despite the plethora of current applications, a critical limitation often exists: cells remain in wells during the entire analysis.[17] As a result, characterizations are typically limited to on-chip fluorescence-based measurements. The utility of microwell arrays, particularly in screening applications, could be significantly expanded if cells of interest could be removed from individual wells for subsequent genetic and phenotypic characterizations. In particular, coupling of "omic" technologies (e.g., 16S rRNA sequencing, whole genome sequencing, RNA-seq, etc.) with microwell array measurements could be enabled if selective extraction of cells from wells and in some cases subsequent enrichment through culture is achieved. For

Received: October 5, 2018
Accepted: December 18, 2018
Published: December 19, 2018

DOI: 10.1021/acsabm.8b00592
ACS Appl. Bio Mater. 2019, 2, 266−276

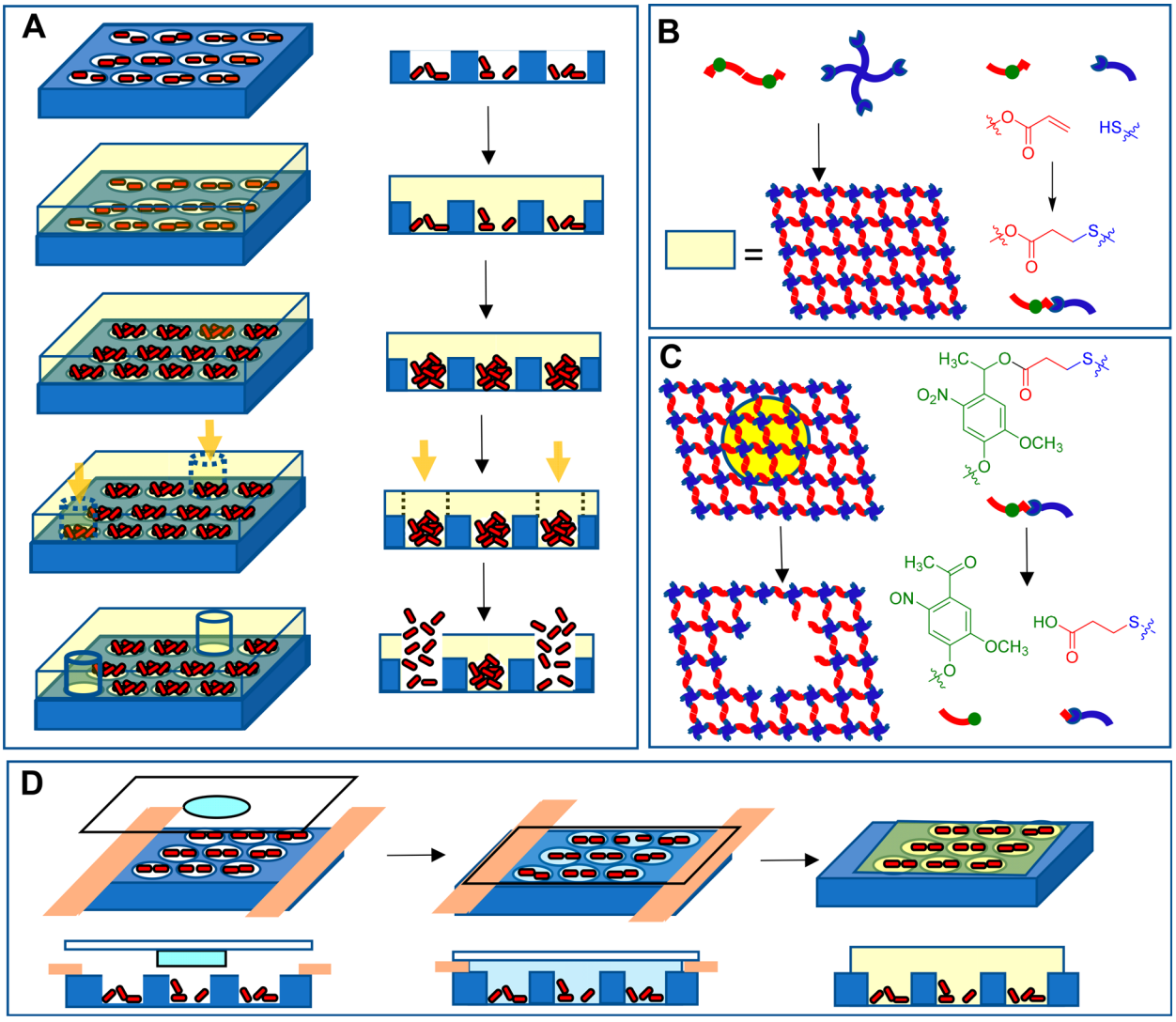

Figure 1. Concept of on demand release and retrieval of bacteria from microwell arrays using a photodegradable membrane. (A) Microwell array (blue) is seeded with fluorescent cells (red) that are confined to the wells by attaching a membrane (yellow) that supports cell growth. Irradiation with light (yellow arrows) degrades the membrane and opens selected microwells after which cells can be retrieved. (B) Photodegradable membrane is made by reacting a four arm PEG-thiol (blue) with a photodegradable PEG diacrylate (red with green dot) by a Michael-type addition reaction. (C) Polymer network of the membrane is degraded when the photodegradable nitrobenzyl group (green) present in the cross-links is cleaved by light (yellow circle) and the polymeric reaction products dissolve in the aqueous medium. (D) To seal seeded cells (red) into microwells with the photodegradable hydrogel, we placed a glass slide with a mixture of the four arm PEG-thiol and PEG-diacrylate (cyan) on top of the seeded microwell with spacers (peach) in between. The membrane precursor solution mixes with the medium (white) inside the wells and cross-links to form the membrane (light blue). After the glass slide is removed, the membrane swells (yellow) when placed in the culture medium.

example, microwells could be used to examine a large number of mutant genotypes for a target phenotype during a mutant library screen but would require subsequent isolation of selected mutants from individual wells for mutation mapping.[17,18]

Hansen and co-workers recently reported a microwell screening platform designed to probe microbe−microbe interactions.[15,19−21] Although this platform had the benefit of high-throughput measurement, it had limited characterization capabilities due to the lack of cell retrieval. Kim and co-workers recently addressed this problem using a manual capillary-driven bacteria retrieval strategy from 100 μm diameter wells.[10] This approach allows for cell retrieval; however, it requires relatively large microwell sizes. Additionally, their strategy makes individual microwells closed systems with limited nutrient flux due to the use of fluorinated oil to compartmentalize the wells. These constraints motivate the development of new materials and interfaces that enable efficient nutrient exchange as well as selective extraction of live cells from microwells at improved spatial resolutions.

In this paper, we outline a new cell retrieval approach using a semipermeable, photodegradable membrane that permits exchange of nutrients and waste products and seals motile bacteria within microwells. The photodegradability of the membrane enables individual wells of interest to be opened using patterned UV light for selective release and retrieval. The proof of concept studies use a light-responsive poly(ethylene glycol) (PEG) hydrogel as a photodegradable membrane and silicon microarrays seeded with the bacterium *Agrobacterium tumefaciens*, the causative agent of crown gall disease in a wide range of plants including apples, walnuts, and sunflowers.[22] As is common among bacteria, the success of this plant pathogen

DOI: 10.1021/acsabm.8b00592
ACS Appl. Bio Mater. 2019, 2, 266−276

is heavily influenced by interactions with other bacteria, many of which are unknown.[23] The platform allows tracking or end-point observation of cell growth based on fluorescence intensity measurement of mCherry-expressing *A. tumefaciens* inside of microwells. Using a light patterning tool, selected microwells can be opened individually or in parallel, thereby allowing subsequent retrieval of viable cells. This material-based approach affords a high degree spatial control over bacteria retrieval and can be adapted to other high-throughput screening formats. For these reasons, we expect that this approach will be a powerful tool for microbiome engineering efforts, as well as other applications where screening or studying cell−cell interactions is important.

2. RESULTS AND DISCUSSION

Concept and Material Selection. A key feature of our strategy for on-demand release of bacteria from microwell arrays is the attachment of a photodegradable membrane (yellow) on a silicon microarray (blue) that confines motile, live cells (red) in the wells (Figure 1A). The membrane forms a physical barrier that prevents bacteria from escaping the microwells but allows diffusion of nutrients, oxygen, and metabolic waste products. The membrane can also be locally degraded by bacteria to generate space for growth within the wells. Light irradiation of selected microwells opens the wells, allowing for retrieval and characterization of the present cells (Figure 1A).

Hydrogels are cross-linked networks of hydrophilic polymers that have a high water content and tend to swell. Hydrogels are widely used for sustained drug delivery systems, tissue engineering applications, nonfouling coatings, and material adsorption.[24] Because of their high water content, biocompatible hydrogels are well-suited for use as the membrane-enclosing bacteria within microwells required for our on demand cell retrieval scheme. Anseth and co-workers[25] reported the development of photodegradable hydrogels using the thiol−acrylate Michael-type addition reaction between functionalized multiarm PEG polymers pioneered by Hubbell et al.[26] The photodegradability of these hydrogels stems from the incorporation of a light-cleavable nitrobenzyl group within their network structure, which allows for a controlled decrease in cross-linking density throughout the network upon light exposure to the point of reverse-gelation. These materials allow for high spatiotemporal control over degradation[27] and are nontoxic to cells,[27,28] and their aqueous nature permits transport of nutrients and waste products[29] to support bacterial cell growth within microwells. For these reasons, we identified photodegradable PEG hydrogels as a good material for use as responsive membranes over microwells. To generate membranes, a step-growth polymerization mechanism that uses a tetra-functional PEG-thiol cross-linker and a photodegradable PEG-diacrylate was used (Figure 1B). A key advantage of this polymerization approach is that it generates hydrogel networks with uniform cross-linking density and microstructure, allowing for uniform diffusion across the array.[25]

Membrane Attachment to the Microwell Array. It was reasoned that the swelling properties of PEG hydrogels, i.e., the increase in volume by adsorption of water, could be used as a means of attaching the membrane to the microwell array. PEG hydrogels are prepared by mixing PEG diacrylate with multiarm PEG thiol at basic pH to form the cross-linked network.[26] This precursor solution can form a thick film on the microwell array and move into the microwells before complete cross-linking and gelation occurs. Upon immersing the microwell array in culture medium, swelling of the cross-linked polymer network can then lock the membrane into place and seal the microwells, preventing motile bacteria from moving out (Figure 2E). Physical attachment of the membrane to the microwell array may be facilitated by the scalloped sidewalls of the microwells resulting from the Bosch etching process.[21] In this way, attachment of the membrane could be achieved without the need for a reactive surface.

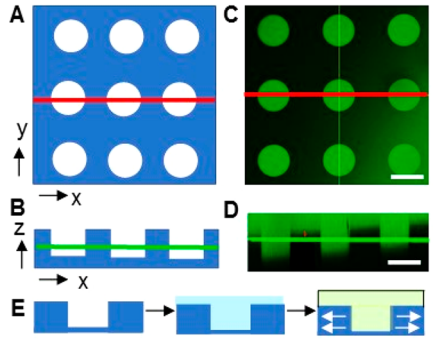

Figure 2. Confocal images of the membrane attached to a microwell array. Schematic representations of the microwell viewed in the (A) *xy* and (B) *xz* planes to aid interpreting the data in C and D. (C) Fluorescence signal, indicating fluorescein labeling of the PEG hydrogel membrane, coming from the *xy* plane along the green line in the xz plot shown in D. (D) Fluorescence signal coming from the xz plane along the red line shown in the *xy* plot in C. (E) Proposed locking mechanism for membrane attachment. The membrane precursor solution mixes with culture medium (white) and cross-links to form the hydrogel (light blue). When placed in culture medium the membrane swells (yellow) creating forces on the walls of the microwells preventing detachment. Microwell size: 100 μm, scale bar: 100 μm, (n = 2).

To test the attachment strategy, we first filled microwells with LB medium and prepared them as shown in Figure 1D. Upon removing the glass slide, the membrane remained firmly attached to the microwells and no membrane movement was observed after incubating the array in LB medium for 2 days (n = 2). The number of microwells per unit surface area appeared to be critical for stable membrane attachment. Microwell arrays with large blank areas, i.e., areas without microwells showed membrane detachment within several hours when placed in LB medium. To verify that membrane attachment occurred through an anchoring mechanism, we used confocal laser scanning microscopy to obtain three-dimensional reconstructions of fluorescently labeled membranes on the microwell arrays (Figure 2C, D). Because of its nonfluorescence, the silicon microwell array appears black whereas the membrane appears green after labeling the membrane with fluorescein (for details see section 4.8 in the Experimental Section). The membrane is present throughout microwells with observed diameters (100 μm) and depths (20 μm) that correspond to well dimensions (Figure 2). Similar results were obtained for microwells with 4, 20, 40, 50, and 60 μm diameters (data not shown). Swelling of the membrane was confirmed by measuring membrane thickness after arrays were placed in LB medium. Hydrogels were observed to be approximately 150 μm thick despite having been polymerized on microwell arrays using 38 μm spacers, suggesting that swelling had occurred.

DOI: 10.1021/acsabm.8b00592
ACS Appl. Bio Mater. 2019, 2, 266−276

Bacteria Can Grow When Encapsulated in the Hydrogel Membrane Material. A potential limitation to attaching the membrane to the microwells via the anchoring mechanism described in the previous section is that the membrane may occupy well space required for bacterial growth. However, these photodegradable PEG hydrogels have ester groups in the cross-links that in theory could be degraded via hydrolysis, as has been reported for ester-containing PEG hydrogels.[30] We reasoned that the presence of the ester structure throughout the hydrogel network should allow for bacteria-dependent network degradation. Consequently, bacteria embedded within the hydrogel membrane should be able to grow within spaces that they create by locally degrading the membrane. To test this, we encapsulated *A. tumefaciens* cells expressing the fluorescent protein mCherry by adding the cells to the membrane precursor solution (Figure S1). After gelation, individual bacteria cells encapsulated within the membrane could be observed by microscopy (data not shown). After 24 h, the membrane itself appeared opaque (Figure S2A, B) indicating that bacteria had grown within the membrane (n = 4). This was confirmed by microscopy which showed the presence of large (20−40 μm) clusters of cells (Figure S2C). These clusters also formed inside membranes prepared at higher thiol/acrylate concentrations (35 mM instead of 22 mM) (Figure 3, Figure S3A, B). Membranes were

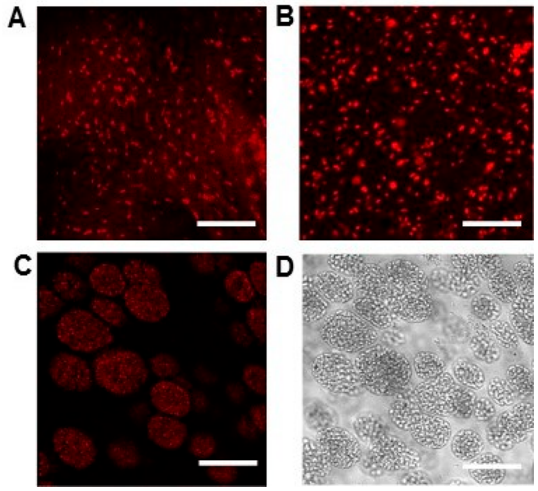

Figure 3. Confocal images of *A. tumefaciens* after encapsulation inside the membranes at different time points. Bacteria in the hydrogel were fixed after (A) 0, (B) 10, and (C) 24 h before acquiring fluorescence confocal images. (D) Bacterial clusters are present in the hydrogel 24 h after encapsulation (differential interference contrast (DIC) image). Thiol concentration: 35 mM, acrylate concentration: 35 mM. Scale bar: 50 μm, (n = 3).

fixed at different time points to see how the initial single bacteria grow into larger clusters over the course of 1 day. To confirm that the bacteria inside these clusters were alive after 24 h, we placed unfixed membranes in LB containing triphenyltetrazolium chloride (TTC).[31] This compound is colorless but is reduced by metabolically active bacteria resulting in the formation of pink, water-insoluble crystals. When TTC was added the membrane turned pink and microscopic observation showed the presence of crystals indicating that the bacteria in the clusters were alive (Figure S3C) (n = 3).

The mesh size of PEG hydrogels is typically in the nanometer range.[30] For this reason, it is unlikely that the space occupied by the observed clusters of bacterial cells (Figure 3) was initially present in the membrane. The presence of the large clusters also suggests that the mesh size of the membrane allows for sufficient mass transfer of nutrients to support bacteria growth. To further investigate mass transfer from the wells, we loaded GFP protein (MW = 27 kDa) into the wells, attached the membrane, and monitored well fluorescence (Figure 4). Although protein aggregation and

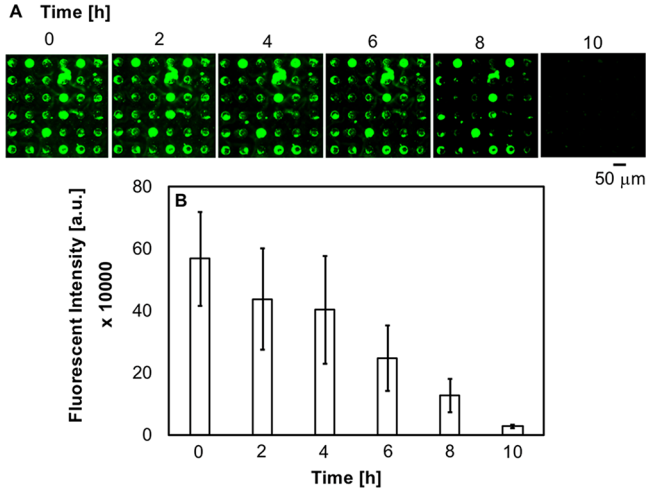

Figure 4. GFP diffusion from the wells. (A) Time-lapse fluorescent images of wells after loading them with GFP, membrane attachment, and soaking in 1X PBS media. (B) Average fluorescence intensity from the wells at each time point.

adsorption to the well walls may impede GFP diffusion, the decrease in well fluorescence intensity over 10 h indicates that the system allows for diffusion of nutrients and large biomolecules. PEG hydrogels formed with higher polymer concentrations and a smaller mesh size[32−34] also supported the formation of large clusters of viable bacteria (data not shown).

Finally, to quantify the effect of the hydrogel on cell growth and metabolic activity, we encapsulated *A. tumefaciens* in the hydrogel and compared its growth to the same number of cells grown in suspension using the TTC assay. Bacteria encapsulated within the hydrogel showed 40% reduction in metabolic activity compared to those grown in suspension (Figure S4). Because TTC measures metabolic activity, this reduction could be explained by lower cell numbers and/or less metabolically active bacteria in the hydrogel compared to those grown in suspension.

Culture of Cells in Microwell Arrays with Attached Hydrogel Membranes. Our platform requires that the photodegradable membrane both prevents cells from leaving microwells and does not interfere with cell growth. Three hours after seeding cells into 20 μm diameter wells, fluorescein-labeling of the hydrogel shows that the membrane is present throughout these microwells with localized spots of higher fluorescence intensity (Figure 5A, left panel). These spots spatially correspond to the location of the seeded bacteria (Figure 5A, middle and right panels). We propose that reaction of fluorescein maleimide with thiol groups present on the bacteria result in cells having fluorescent signal in both the green and red channels. To show that the bacteria can grow with the membrane attached to the array, we seeded *A.*

DOI: 10.1021/acsabm.8b00592
ACS Appl. Bio Mater. 2019, 2, 266−276

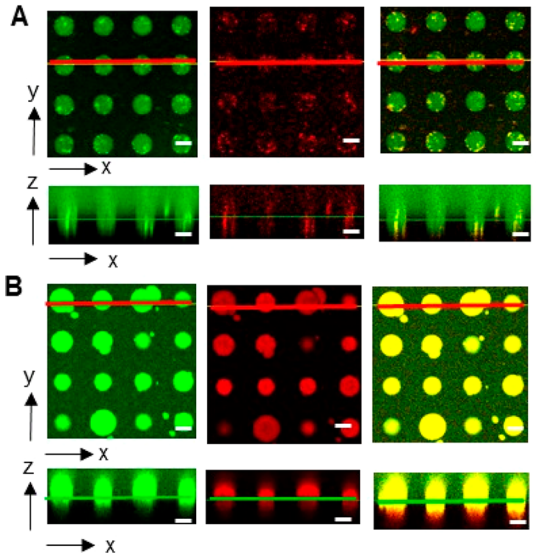

Figure 5. Confocal images of *A. tumefaciens*-seeded microwell array with an attached hydrogel membrane. (A) Fluorescence intensities 3 h after cell seeding coming from the *xy* plane along the green line and the *xz* plane along the red line. Left panel green fluorescence fluorescein-labeled membrane; middle panel red fluorescence of the bacteria; right panel overlay of both. (B) Same as A but after culturing for 24 h. Samples were fixed prior to measurements. Well diameter, 20 μm; seeding OD = 0.2; scale bar = 20 μm, n = 5.

tumefaciens at the same optical density but kept the microwell immersed in medium for 24 h. Consistent with bacterial growth, there is an increase in the red fluorescence signal following this incubation (Figure 5B, middle panel). Further, bacteria are present above the silicon/membrane interface (Figure 5B, middle and right panels). Although 38 μm spacers were used during hydrogel preparation, the thickness of the membrane is much greater due to swelling of the membrane in the culture medium (approximately 150 μm thick). Bacteria are present approximately 40 μm above this interface, indicating that bacteria invade the membrane. However, membrane degradation appears to occur mainly in the *z*-direction, with relatively little degradation occurring in the x and *y*-directions (Figure S5). For this reason, we observe no mixing between neighboring wells over the 24 h time period required for growth (Figure 5B). Although we did not observe mixing of cells from neighboring wells in our experiments, this might not be the case for other bacterial strains or experimental conditions. For this reason, use of this platform may require optimization of experimental conditions such as bacteria seeding density or further optimization of microwell design.

In summary, these observations indicate that the membrane polymerized over a seeded microwell array serves as an effective barrier that compartmentalizes the microwells while allowing bacteria to proliferate inside of the microwells—a critical requirement when screening for growth or growth inhibition. The process of attaching the membrane and observing growth is robust and has been carried out many times (n = 22). Although we have not experimentally determined an upper limit of assay time, based on the degree of membrane degradation observed after 24 h (≈ 40 μm) and the membrane thickness (≈ 150 μm) it is estimated that the membrane should be operational for at least 3 days in its current configuration.

Membrane Photodegradation and Cell Release. The ability to selectively open microwells is critical for our application. To demonstrate this, we used patterned illumination with the Polygon400 to degrade the membrane over, and thereby open, targeted 45 μm diameter microwells (Figure 6). To confirm membrane degradation has occurred

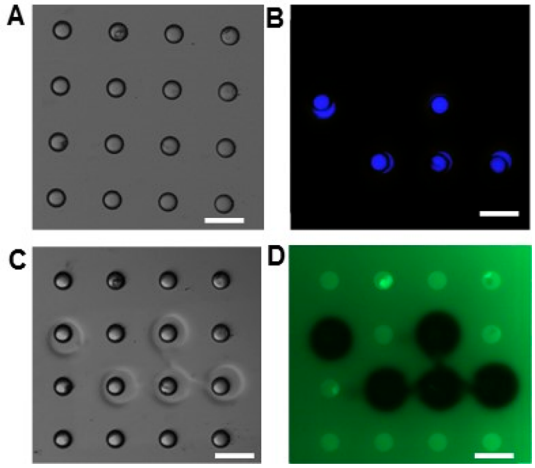

Figure 6. Microwells can be opened by degrading the membrane with light. (A) 45 μm wells after membrane attachment, (B) patterned light during irradiation (blue), (C) after irradiation (D) and after labeling with fluorescein maleimide. Exposed area, 50 μm diameter circle; irradiation time, 5 min; light output, 1.4 mW/mm^2; scale bar = 100 μm; n = 3.

only in irradiated areas, we labeled the membrane with the thiol-reactive fluorescein maleimide dye and observed by fluorescence microscopy. As expected, irradiated areas are devoid of fluorescent signal indicating that polymer network degradation is localized to directly irradiated areas.

To demonstrate the ability to release bacteria from microwells, we seeded *A. tumefaciens* in 60 μm wells, allowed them to grow for 2 days, and then irradiated the membrane with light (Figure 7). As expected, the polymer network

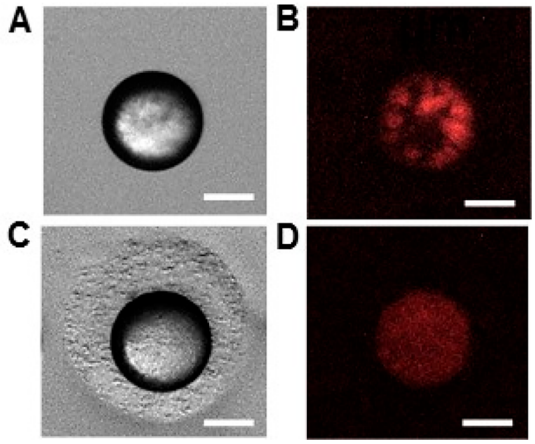

Figure 7. Membrane degradation of bacteria-seeded microwells leads to bacteria release. Bright-field and fluorescence images (A, B) before and (C, D) after irradiating a 60 μm microwell with the Polygon400. *A. tumefaciens* was seeded at OD = 0.2 and cultured for 2 days. Exposed area, 120 μm circle; irradiation time, 5 min; light output, 2 mW/mm^2; scale bar = 30 μm.

DOI: 10.1021/acsabm.8b00592
ACS Appl. Bio Mater. 2019, 2, 266−276

degrades, opens the microwells, and releases cells. A few minutes after light exposure, bacteria move to the irradiated area next to the microwell (Figure 7C), whereas other cells stay in the microwell (Figure 7D) (n = 6). Notably, localized clusters of cell fluorescence present within microwells prior to irradiation (Figure 7B) are no longer visible after irradiation. Instead the fluorescence signal observed within irradiated microwells appears diffuse, suggesting that cells remaining in wells are no longer structured into clusters by the hydrogel (Figure 7D). Thus, under these experimental conditions *A. tumefaciens* cell clusters appear to be readily removed upon light exposure, corresponding to the release of bacteria. This may not be true for all experimental conditions or bacteria, and so additional sample processing may be necessary in cases where bacteria remain as stable cell clusters or biofilms after irradiation.

The Polygon400 allows spatiotemporal control over membrane degradation. To examine how irradiation time at a fixed light intensity impacts bacteria release from 20 μm diameter microwells, we irradiated adjacent microwells for 1, 2, 3, 4, or 5 min (Figure 8A). Cells were observed moving out of

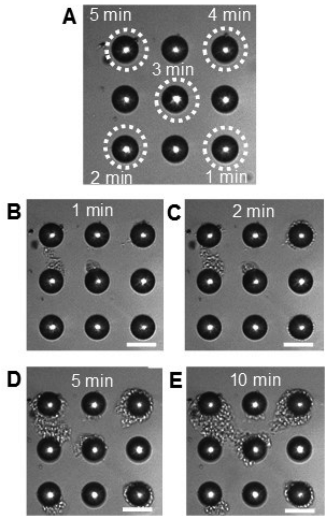

Figure 8. Effect of irradiation time on bacteria release from 20 μm diameter wells. (A) Wells were irradiated as indicated for either 1, 2, 3, 4, or 5 min and afterward (B–E) observed over the course of 10 min. Light output 0.7 mW/mm^2. Scale bar = 25 μm, n = 2.

all of these wells by 5 min after irradiation (Figure 8D), however cells were observed exiting microwells that were irradiated for longer periods of time only 1 or 2 min after irradiation (Figure 8B, C).

A benefit of this method is that any number and combination of wells can be simultaneously opened, enabling parallel extraction of cell populations, if desired. To demonstrate this, ten nearby 50 μm diameter microwells were simultaneously irradiated using the Polygon400 (Figure 9A, B), resulting in cell release (Figure 9C, E) and membrane degradation (Figure 9D, F) from each targeted well. The cell-dependent fluorescence signal drops to background levels after washing the microwells with LB medium showing that the bacteria can be removed (Figure 9E). The release of bacteria can be semiquantified by measuring the fluorescence intensity from the individual wells before and after opening. The fluorescence intensity of opened wells decreases by about 60%

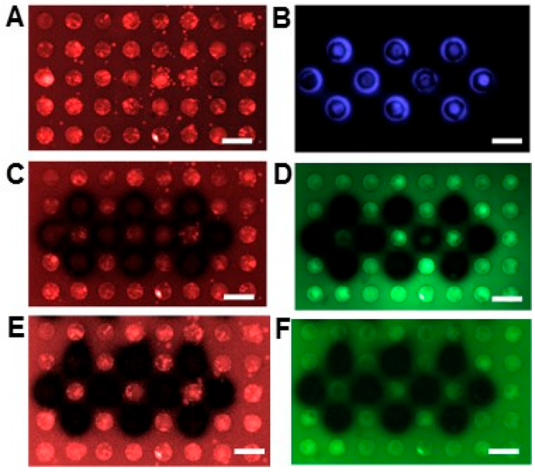

Figure 9. Several wells can be opened simultaneously using the Polygon400. (A) *A. tumefaciens* expressing fluorescent mCherry was seeded at OD = 0.2 and cultured for 1 day. (B) Simultaneous irradiation of ten 50 μm microwells with a 60 μm circle pattern for 5 min at 0.7 mW/mm^2. (C) Microwells that were irradiated show diffuse red fluorescence due to the moving bacteria. (D) Fluorescein maleimide labeling confirms membrane degradation. (E, F) Same as C and D but after washing with LB medium. Scale bar = 100 μm. Simultaneous opening of multiple wells has been done numerous times (>20).

(Figure S6), consistent with our observations of cells are leaving the microwells after irradiation. After the wells are washed, the fluorescence intensity of opened wells drops by another 30%, suggesting that most cells can be removed.

Retrieval of Bacterial. To verify that bacteria from selected wells can be harvested from wells and cultured for follow-up analysis, opened wells were washed with an extraction medium. Washing after well opening is an easy and straightforward approach to retrieve cells. Additionally, this approach allows easy verification that bacteria have been extracted by using a microscope to inspect washed microwell arrays (e.g., Figure 9E). To show that we can retrieve bacteria from selected microwells, 72 microwells (40–50 μm in diameter) were opened in four different runs (Figure S7). The arrays were then washed with extraction medium (LB with 0.05% Tween20) to remove the bacteria from the microwells. To show that the bacteria were viable and could be enriched, the washings were cultured overnight in a polystyrene well plate. As a control to show that the isolated bacteria originate from the opened microwells, the microwell array was also washed with the same volume of extraction medium prior to the well opening. The washings taken from opened wells showed bacteria growth, as measured by the increase in OD at 600 nm. In contrast, the control washings taken from wells prior to opening did not increase in OD over time (Figure 10A). This suggests that the bacteria cultured from washings after well opening originated from the opened microwells. Because the observed OD increase is only qualitative, we repeated the experiment and plated the washing solutions on agar to quantify cell density (Figure 10B). Colony forming units per mL (CFU/mL) were approximately 1000-fold higher in the extract after opening ten wells. This suggests that >99.9% of the cells present in the extract originated from the wells. These results demonstrate that under these experimental conditions *A. tumefaciens* cells can be retrieved from the microwells and remain sufficiently viable to be cultured for

DOI: 10.1021/acsabm.8b00592
ACS Appl. Bio Mater. 2019, 2, 266–276

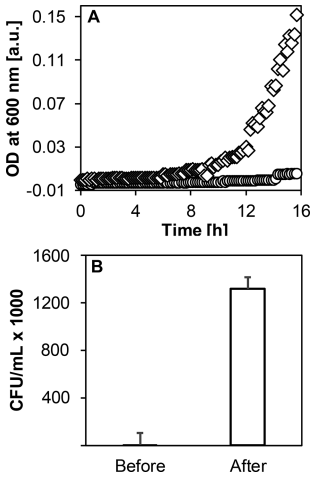

Figure 10. *A. tumefaciens* isolated from microwells are viable and can be cultured. (A) Total of 72 microwells (40−50 μm in diameter) were opened with light. After careful washing of the membrane with LB with 0.05% Tween20, the solution was placed inside a plate reader and the OD tracked over time. Washings after opening the microwells (rhombus) show an increase in OD over the course of 16 h whereas washings before opening the microwells (circles) do not show bacterial growth (n = 3). (B) Quantification of bacteria colony forming units (CFU/mL) present in the washing solutions before and after opening of ten 50 μm diameter wells (n = 3).

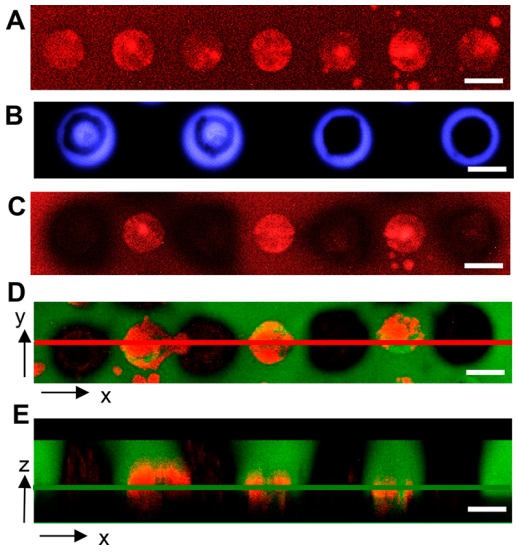

Figure 11. Effect of light pattern on bacteria removal from microwells after culture for 1 day (OD = 0.2 seeding density). (A) 40 μm microwells containing bacteria were (B) irradiated either with 60 μm light circle or 60/40 μm light ring patterns (blue) for 5 min at 0.7 mW/mm^2. (C) Cells are released as shown by the diffuse red fluorescence. After washing, the membrane is fixed and imaged by confocal microscopy. (D) Fluorescence signal (green indicating fluorescein-labeled membrane, red indicating cells expressing mCherry) coming from the *xy* plane along the green line in E. (E) Fluorescence signal coming from the xz plane along the red line in D. Scale bar = 40 μm. Effect of ring versus circle irradiation on cell release was done in triplicate.

follow-up analysis. However, irradiation may problematically reduce cell viability when experiments use other bacterial strains or experimental conditions. Accordingly, use of this platform under other conditions may require the optimization of irradiation time, membrane thickness, or other design features to maintain cell viability through the extraction and retrieval procedure.

Avoiding Direct Exposure of Bacteria to UV Light. A well-recognized problem in applications using light for manipulation of cells is its effects on cell viability and behavior.[35] The use of a two-photon process for cleavage of the nitrobenzyl group has been reported and can be used to avoid this problem .[36] However, we found that projecting light in ring patterns with an inner diameter corresponding to the diameter of the well can also release bacteria from the wells while avoiding direct UV exposure (Figure 11A−C). Here, the membrane surrounding the perimeter of the well is removed, and the remaining membrane island likely diffuses into solution. This has the advantage that the bacteria inside the wells are not directly exposed to UV light, thereby reducing its effect. We found that irradiation of 40 μm diameter microwells with either full light circles or light ring patterns resulted in loss of the membrane above the wells (Figure 11D). In both cases, cells in targeted wells were released as observed by the diffuse mCherry fluorescence patterns (Figure 11C). Confocal microscopy after washing the wells (Figure 11D, E) confirmed that the bacteria were released for both light patterns. The ability to illuminate only the well perimeter is a critical feature of this approach, allowing the user to illuminate the surface with higher intensities and longer exposure times if necessary.

3. CONCLUSIONS

The retrieval capabilities demonstrated here connect the high-throughput screening benefits inherent to microwell array formats with the ability to extract, isolate, and enrich cells from any well of interest to determine molecular or phenotypic information about that cell population. The approach has potential to be used forfollow-up characterizations on cell populations that show a desired and/or rare function. Follow-up assays could include but are not limited to whole genome sequencing, a variety of cellular functional assays, discovery of new strains or genotypes, and identification of genetic determinants of key phenotypes.

The proof-of-principle studies demonstrated here show that the photoresponsive membrane attaches to microwell substrates, confines bacteria while allowing for nutrient exchange and cell growth, and is degradable with patterned light for cell release and retrieval from any well of interest at high (20 μm) spatial precision. Key design features are the presence of the photoreactive nitrobenzyl group, allowing for polymer network degradation, thereby opening the wells in a spatially controlled manner using the Polygon400 pattern illumination instrument, and the ability to avoid direct exposure of cells to UV using patterned ring illumination. In our laboratory, these methodological advancements will be used for screening, 16S rRNA sequencing, and identification of environmental microbes with antagonistic or synergistic impacts on bacteria of key functional importance, such as *A. tumefaciens* and other pathogens. Although our focus is on bacteria, the platform and method should be amendable for applications involving mammalian cells as well.

4. EXPERIMENTAL SECTION

4.1. Instrumentation. *4.1.1. Bright-Field and Fluorescence Microscopy.* All images were taken with an upright (BX51, Olympus Japan) microscope equipped with a 3S camera (Luminara, Ottawa, ON, Canada) controlled by the Infinity Capture Software unless otherwise stated. For experiments involving the Polygon400 (Mightex

DOI: 10.1021/acsabm.8b00592
ACS Appl. Bio Mater. 2019, 2, 266−276

Systems), the camera was controlled by the Mightex Polyscan2 software. Greyscale images were processed and colored using ImageJ software[37] for visualization: blue for Polygon400 light patterns, red for mCherry, and green for fluorescein.

4.1.2. Confocal Laser Scanning Fluorescence Microscopy (CLSFM). Fluorescent images were acquired on an Olympus FluoView FV1000-D confocal laser scanning fluorescence microscope equipped with 473 and 559 nm lasers and controlled by Fluoview software.

4.1.3. Polygon400 Light Patterning Instrument. Light patterns were projected onto the membrane using the Polygon400 instrument attached to the BX51 upright microscope via an adapter containing a dichroic/filter cube. The 365 nm high-power LED source (50 W) was controlled by a BioLED light source control module and delivered to the Polygon400 with a liquid light guide (Figure S8). A BioLED analog and digital I/O control module provided computer control and TTL trigger when used with the LED controller. Size and shape of the pattern, light intensity as well as irradiation time were controlled with the Mightex PolyScan2 software. Approximate light intensities for the 10×/0.3NA and 20×/0.5NA objectives according to the manufacturer are 7 and 20 mW/mm^2, respectively, with the LED source at maximum intensity (100%). Prior to each experiment, the Polygon400 was calibrated with a mirror and the calibration software.

4.1.4. Measurements of Optical Densities and Growth Curves. Optical densities (OD) of bacteria cultures (100 μL) at 600 nm were measured in 96 well plates on an Epoch2 microplate reader (Biotek). Time course experiments were done by measuring the OD at 600 nm using 100 μL of bacteria suspension in 96 well plates with a cover at 28 °C and with continuous orbital shaking at 237 cpm (cycles per minute).

4.1.5. ^{1}H NMR Spectroscopy. ^{1}H NMR spectra were recorded on a Varian Mercury 400 MHz or Varian System 500 MHz spectrometer in deuterated chloroform ($CDCl_3$) or dimethyl sulfoxide (d_6-DMSO). The number of scans was 32−64 and the D1 was 1 s for small compounds and 10 s for polymers.

4.1.6. Plasma Cleaner. The plasma cleaner was a PDC-001-HGP instrument (Harrick Plasma).

4.1.7. pH Meter. The pH of solutions was measured with an Oakton pH 700 instrument.

4.2. Materials. *4.2.1. Chemical Reagents.* *N*-hydroxy succinimide (NHS), dicyclohexyl carbodiimide (DCC) and poly(ethylene glycol) (PEG)-diamine (MW 3400), deuterated chloroform ($CDCl_3$), dimethyl sulfoxide (d_6-DMSO), phosphorpentoxide (P_4O_{10}), sodium phosphate dibasic (NaH_2PO_4), Alconox detergent, 4A molecular sieves, sodium hydroxide (NaOH), triethylamine (Et_3N), trichloro-(1*H*,1*H*,2*H*,2*H*-perfluorooctyl)silane, 1 M HCl (aq), and anhydrous toluene were purchased from Sigma-Aldrich. Four arm PEG-thiol (MW 10000) was purchased from NOF America Corporation. Dimethylformamide (DMF), ethanol (EtOH), dichloromethane (CH_2Cl_2), ethyl acetate (EtOAc), diethyl ether (Et_2O), sodium hydrogen sulfate ($NaHSO_4$), anhydrous magnesium sulfate ($MgSO_4$), and isopropanol were purchased from Fisher. Fluorescein maleimide was purchased from Cayman. All chemicals were used as received unless stated otherwise. CH_2Cl_2 and Et_3N were dried over 4A molecular sieves. NB-COOH (for chemical structure see Scheme S1) was prepared in five steps starting from acetovanillone following reported procedures.[27,38,39] The ^{1}H NMR chemical shifts in $CDCl_3$ or d_6-DMSO for all intermediates were consistent with reported ^{1}H NMR chemical shifts.

4.2.2. Bacteria Culture. Tryptone soy agar, yeast extract, kanamycin, isopropylthiogalactoside (IPTG), triphenyltetrazolium chloride (TTC), Tween20, and sodium chloride (NaCl) were purchased from Sigma-Aldrich. *A. tumefaciens* C58 pSRKKm-mCherry was prepared using established electroporation methods.[40] This plasmid carries the gene encoding the fluorescent protein mCherry under control of the *lac* promoter allowing for IPTG induction of mCherry expression.[41]

4.3. Synthesis of the Photodegradable Poly(ethylene glycol) PEG Diacrylate. The synthesis of this polymer has been reported[27] and was prepared in a different way by reacting PEG-diamine with the *N*-hydroxysuccinimide ester of the nitrobenzyl carboxylic acid as outlined in Scheme S1.

NB-NHS. NB-COOH (251.6 mg, 0.71 mmol) and 82.0 mg of (0.71 mmol) of NHS were dissolved in a mixture of 2 mL of DMF and 4 mL of CH_2Cl_2. The solution was cooled at 0 °C for 25 min before a solution of 146.9 mg (0.71 mmol) of DCC in 2 mL of CH_2Cl_2 was added. The mixture was stirred for 19 h. The suspension was concentrated in a flow of nitrogen and filtered through a plug of glass wool inside a glass Pasteur pipet. The residue was washed with 2 mL of EtOAc and the filtrate diluted to 25 mL with the same solvent. The yellow solution was washed with water (3 × 25 mL), dried over $MgSO_4$, and concentrated in a flow of nitrogen. The solid was dried under reduced pressure to yield NB-NHS as a yellow solid in quantitative yield. ^{1}H NMR ($CDCl_3$) δ = 7.60 (s, 1H, CH_{aromat}), 7.01 (s, 1H, CH_{aromat}), 6.54 (m, 1H, CH), 6.43 (d, 1H, CH = CH_{trans}), 6.17 (dd, 1H, C$\underline{H}$=CH_2), 5.87 (d, 1H, CH = CH_{cis}), 4.16 (t, 2H, CH_2O), 3.91 (s, 3H, OCH_3), 2.88 (t, 2H, CH_2CO), 2.84 (s, 4H, $COCH_2CH_2CO$), 2.29 (m, 2H, $CH_2C\underline{H}_2CH_2$), 1.66 (d, 3H, CH_3CH).

Photodegradable PEG Diacrylate. NB-NHS and PEG-diamine were dried under reduced pressure in the presence of P_4O_{10} at 40 °C to constant weight; 317.8 mg (0.71 mol, 4.2 equiv (eq) relative to amine) of NB-NHS was dissolved in 2 mL of CH_2Cl_2 and to the slightly hazy solution was added over the course of 5 min a solution of 290 mg (0.085 mmol, 0.17 mmol amine groups) of PEG-diamine and 29.7 μL (0.21 mmol) of Et_3N in 5 mL of CH_2Cl_2. The mixture became clear and was stirred in the dark at room temperature. After 23 h, the solution was concentrated in a flow of nitrogen and the residue suspended in 2 mL of CH_2Cl_2. The mixture was filtered and the residue washed with CH_2Cl_2 (2 × 2 mL). The filtrate was diluted with 100 mL of Et_2O to precipitate the polymer that was recovered by filtration through a glass filter. The residue was dissolved in 25 mL of 1 M $NaHSO_4$ (aq) and filtered (0.22 μm). The clear solution was extracted with CH_2Cl_2 (3 × 25 mL), dried over $MgSO_4$, and concentrated in a flow to a volume of 6 mL. This solution was diluted with 100 mL of Et_2O to precipitate the polymer. The polymer was recovered by filtration, dissolved in 8 mL CH_2Cl_2 and diluted with 100 mL of Et_2O. The precipitate was filtered, dried under reduced pressure to yield 267.1 mg of a faint yellow solid. ^{1}H NMR ($CDCl_3$) δ = 7.58 (s, CH_{aromat}), 6.99 (s, 1H, CH_{aromat}), 6.51 (m, CH + NH), 6.42 (d, CH = CH_{trans}), 6.15 (dd, C$\underline{H}$=CH_2), 5.86 (d, CH = CH_{cis}), 4.10 (t, CH_2O), 3.92 (s, OCH_3), 4.18−3.26 (CH_2CH_2O), 2.38 (t, CH_2NH), 2.16 (m, $CH_2C\underline{H}_2CH_2$), 1.64 (d, CH_3CH). The degree of functionalization for a MW = 3400 was 80% by comparing the integral ratios of the aromatic and CH_2CH_2 PEG protons. This degree of functionalization was considered when preparing the aqueous stock solutions.

4.4. Microwell Fabrication. Microwell arrays were fabricated to contain a parylene liftoff mask to allocate cells in microwells while eliminating background cells, according to the procedures outlined in Hansen et al.[21] Arrays were designed to contain wells with diameters ranging from 8 to 200 μm at different pitches.

4.5. Bacteria Culture. LB medium was supplemented with 150 μg/mL kanamycin and 0.5 mM IPTG and prepared fresh for each experiment from frozen stocks stored at −20 °C. Under laminar flow a frozen 25% glycerol stock of *A. tumefaciens* was inoculated in 2 mL LB medium in round-bottom borosilicate glass tubes (13 mm × 100 mm, 10 mL, Globe Scientific). The culture tubes were closed with Bacti-caps (Clark Scientific) having openings to provide oxygen at atmospheric conditions inside the tube. Cultures were grown at 28 °C for 22 h by shaking at 200 rpm. After spinning down at 2000 g for 10 min the bacteria pellet was suspended in medium and diluted 1:250 in fresh medium (culture volume 2 mL). After 11 h at 28 °C and 200 rpm, the bacteria reached mid log phase and the culture had a typical OD of 0.2 (100 μL). The bacteria were spun down at 2000 g for 10 min and resuspended in 100 μL of fresh LB medium at the desired OD.

4.6. Membrane Fabrication. *4.6.1. Cross-Linking Buffers.* Phosphate buffered saline LB pH8 was prepared by adding NaH_2PO_4 to LB and adjusting the pH of the solution with 5 M

DOI: 10.1021/acsabm.8b00592
ACS Appl. Bio Mater. 2019, 2, 266−276

NaOH (aq). The final phosphate concentration was 100 mM. This solution was sterile filtered (0.22 μm), lyophilized, and dissolved in half the volume of ultrapure water to make the 2× LB phosphate buffer solution used for membrane fabrication.

4.6.2. Membrane Precursor Solutions. Solutions of four arm-PEG thiol and photodegradable PEG diacrylate in ultrapure water were sterile filtered (0.22 μm), aliquoted, lyophilized and stored at −20 °C for long-term use. Working solutions were prepared by dissolving aliquots in water to give four arm PEG thiol and photodegradable PEG diacrylate solutions with concentrations of 20 and 49 mM,[25] respectively, and stored at −20 °C until use. Because of the high PEG concentration, the amount of water added to make the solutions was corrected by subtracting the volume of PEG calculated from the amount dissolved assuming a PEG density of 1 g/mL.

4.6.3. Perfluoroalkylated Glass Slides. Five glass slides 25 × 75 × 1 mm (Fisher Scientific) were washed with 20 mL of a 2% w/v Alconox solution for 20 min with sonication inside a polypropylene slide mailer. Slides were then washed with ultrapure water (3 × 20 mL) and finally sonicated in water (20 mL) for 20 min. Slides were blown dry with nitrogen and both sides plasma treated for 2 min in air at 800 mTorr with the RF power set to high output (45 W). The slides were placed inside a slide mailer and 20 mL of 0.5% v/v of trichloro(1*H*,1*H*,2*H*,2*H*-perfluorooctyl)silane in toluene was added. After 3 h at room temperature, the slides were washed with toluene (3 × 20 mL) and EtOH (3 × 20 mL) and dried by blowing nitrogen. Slides prepared in this way were easier to separate after membrane preparation compared to slides prepared by chemical vapor deposition under reduced pressure inside a vacuum desiccator. For long-term storage, the slides were kept in 70% isopropanol.

4.6.4. Spacers to Control Membrane Thickness. Initial thickness of the membrane was controlled in the range 38 to 102 μm using steel thickness feeler gage poc-kit assortment blades (Precision Brand).

4.6.5. Encapsulation of A. tumefaciens Inside the Membrane. Bacteria in the mid log phase were diluted to an OD of 0.2 (100 μL). The cell suspensions were spun down in a 500 μL Eppendorf tube and resuspended in the same volume of 2× LB phosphate buffer after supernatant removal. To 12.5 μL of bacteria suspension was added 5.6 μL of the photodegradable PEG diacrylate and the suspension was carefully mixed with the pipet, before 6.9 μL of the four-arm PEG thiol solution was added.[25] After careful mixing the mixture was pipetted (e.g., 4 × 6 μL) onto a glass slide having 102 μm spacers on opposite sides (Figure S1). A second glass slide was placed on top and left for 25 min at room temperature for thiol−acrylate cross-linking and subsequent hydrogel formation. After carefully separating the slides, membranes were washed with LB (5 × 1 mL) to remove nonencapsulated bacteria. The membranes were then placed inside a 24-well plate in 2 mL of LB and cultured in the incubator at 28 °C without shaking.

4.6.6. Cell Viability Assay. TTC was dissolved in LB medium at 5 mg/mL and diluted 10-fold into LB medium containing the hydrogel.

4.6.7. Membrane Fabrication on Microwells Directly. The microwell array was layered with 600 μL of medium and placed inside a desiccator. A vacuum was applied for 30 min to replace air trapped inside the wells with LB medium (Figure S9). For experiments without bacteria the surface was blotted at the sides with Kimwipes tissue paper and the parylene carefully removed using Scotch tape.[21] For experiments with *A. tumefaciens*, the wells were inoculated with 600 μL of a bacteria suspension (OD = 0.2). After 1 h the bacteria suspension was removed with a pipet and the array carefully blotted with a Kimwipe before removing the parylene with Scotch tape. For microarrays without parylene coating, bacteria could also be removed with a PDMS slab after seeding.[10] Immediately after cell seeding, 12.5 μL of 2× LB phosphate buffer was mixed with 5.6 μL of the photodegradable PEG diacrylate and 6.9 μL of the four-arm PEG thiol, then 15 μL of the mixture pipetted onto a glass slide. The glass slide was inverted and placed on top of the microwell array having two 38 μm spacers on opposite sides (Figure 1D) and incubated at room temperature for 25 min for hydrogel formation. After careful separation of the glass slide from the microwell array, the membrane-covered microwell array was placed inside a rectangular well made of polydimethylsiloxane on a glass slide containing 1−2 mL of LB medium (Figure S10) and kept inside the incubator at 28 °C without shaking. This setup prevented drying up of the membrane and enabled easy handling of the microwell array on the microscope stage.

4.7. Membrane Degradation with the Polygon400. The microarray with membrane was kept in LB medium during the experiments in order to prevent membrane dehydration and to dissipate local heating due to the LED light. In addition, immersion in the medium allowed PEG products cleaved from the membrane to solubilize and diffuse away from the wells during irradiation. The Polygon400 tool allows for exposure of a user-defined pattern light in any shape within the working area of the objective, as well as control of light intensity and irradiation time.[42,43] Light patterning experiments were done using 10× and 20× objectives, corresponding to (maximum) rectangular working areas of 330 μm × 590 and 165 μm × 295 μm, respectively.

4.8. Fluorescent Labeling of the Membrane. After light exposure, membranes were visualized by fluorescence microscopy by coupling pendant thiol groups with fluorescein maleimide.[44] 20 μL of a 10 mM stock solution of fluorescein maleimide in DMF was added to the microwell array in 1 mL of LB. This reaction occurs in the pH range 6.5−7.4 and was therefore done directly in LB (pH 6.7). Labeling was typically done for 2 h or overnight. Before image collection, the membrane was washed with LB (3 × 1 mL) to remove unreacted fluorophore.

4.9. Fixing Bacteria Inside the Membrane and Microwells. The bacteria were fixed in 2.5% glutaraldehyde and 2.5% formaldehyde overnight in LB and washed with LB (3 × 1 mL) before the confocal microscope measurements.

4.10. Retrieval of Live Bacteria from Membrane-Covered Microwell Arrays. *A. tumefaciens* was seeded at OD = 0.2 (100 μL), washed with LB medium (2 × 5 mL), placed inside a polystyrene Petri dish, and cultured for 24 h in 5 mL LB medium at 28 °C without shaking. The array was washed (2 × 5 mL) with extraction medium (0.05% Tween20 in LB) to remove any bacteria that could be present outside the membrane, and placed inside the sample holder. The array was again washed in the sample holder with extraction medium (4 × 2 mL) using a pipet. The washings were spun down at 2000 g for 10 min and the supernatant carefully removed leaving 1 mL inside the culture tube. This sample served as the negative control. The microarray was immersed in 1 mL extraction medium and a total of 72 wells were opened in four different runs. After the experiment, another 1 mL of extraction medium was added and the wells washed by pipet. After transferring the washing to a culture tube the microwell array was washed with additional extraction medium (3 × 2 mL). The washings were combined and spun down at 2000 g for 10 min and the supernatant carefully removed leaving 1 mL inside the culture tube. After suspending with the pipet, a volume of 100 μL of retrieved bacteria and 100 μL of the negative control were placed inside the well plate and the OD at 600 nm was measured as a function of time inside a plate reader. The remaining (0.9 mL) solutions were placed inside an incubator at 28 °C and shaken at 200 rpm.

■ ASSOCIATED CONTENT

Supporting Information

The Supporting Information is available free of charge on the ACS Publications website at DOI: 10.1021/acsabm.8b00592.

Schemes for chemical synthesis; setup to encapsulate bacteria in hydrogels; microscope pictures of bacteria-encapsulated hydrogels; assays for bacteria viability in hydrogels; image of the sample holder for the polygon experiment; microscope image of 72 opened microwells; photograph of the Polygon400 setup; comparison of *A. tumefaciens* growth in hydrogels and in suspension; quantification of membrane invasion by *A. tumefaciens*; quantification of *A. tumefaciens* release from microwells (PDF)

DOI: 10.1021/acsabm.8b00592
ACS Appl. Bio Mater. 2019, 2, 266−276

AUTHOR INFORMATION

Corresponding Authors

*Email: tgplatt@ksu.edu. Telephone +1-785-532-6280.
*Email: rrhansen@ksu.edu. Telephone +1-785-532-0625.

ORCID

Ryan R. Hansen: 0000-0002-6471-047X

Notes

The authors declare no competing financial interest.

ACKNOWLEDGMENTS

We acknowledge support from the National Science Foundation under Grant 1650187 and Kansas State University. P.A.N. acknowledges support from the National Science Foundation Graduate Research Fellowship under Grant No. GGVP004842. We would like to thank Dr. Urara Hasegawa (Chemical Engineering Department, Kansas State University) for help with confocal microscopy and use of her equipment for chemical synthesis, Dr. Alvaro Herrera (Biomolecular NMR Facility, Kansas State University) for measuring ^{1}H NMR, Prof. Douglas McGregor and the S.M.A.R.T. lab (Mechanical and Nuclear Engineering, Kansas State University) for microwell fabrication, and Prof. Christopher Bowman (Chemical and Biological Enigneering, University of Colorado) for fruitful discussion.

REFERENCES

(1) Forslund, E.; Guldevall, K.; Olofsson, P.; Frisk, T.; Christakou, A.; Wiklund, M.; Önfelt, B. Novel Microchip-Based Tools Facilitating Live Cell Imaging and Assessment of Functional Heterogeneity within NK Cell Populations. *Front. Immunol.* **2012**, *3*, 300.

(2) Ostuni, E.; Chen, C. S.; Ingber, D. E.; Whitesides, G. M. Selective Deposition of Proteins and Cells in Arrays of Microwells. *Langmuir* **2001**, *17*, 2828−2834.

(3) Rettig, J. R.; Folch, A. Large-Scale Single-Cell Trapping and Imaging Using Microwell Arrays. *Anal. Chem.* **2005**, *77*, 5628−5634.

(4) Li, X.; Chen, W.; Li, Z.; Li, L.; Gu, H.; Fu, J. Emerging Microengineered Tools for Functional Analysis and Phenotyping of Blood Cells. *Trends Biotechnol.* **2014**, *32*, 586−594.

(5) Keymer, J. E.; Galajda, P.; Muldoon, C.; Park, S.; Austin, R. H. Bacterial Metapopulations in Nanofabricated Landscapes. *Proc. Natl. Acad. Sci. U. S. A.* **2006**, *103*, 17290−17295.

(6) Gong, Y.; Ogunniyi, A. O.; Love, J. C. Massively Parallel Detection of Gene Expression in Single Cells Using Subnanolitre Wells. *Lab Chip* **2010**, *10*, 2334−2337.

(7) Chen, Y.; Li, P.; Huang, P.-H.; Xie, Y.; Mai, J. D.; Wang, L.; Nguyen, N.-T.; Huang, T. J. Rare Cell Isolation and Analysis in Microfluidics. *Lab Chip* **2014**, *14*, 626−645.

(8) Moeller, H.-C.; Mian, M. K.; Shrivastava, S.; Chung, B. G.; Khademhosseini, A. A Microwell Array System for Stem Cell Culture. *Biomaterials* **2008**, *29*, 752−763.

(9) Lee, J. M.; Park, D. Y.; Yang, L.; Kim, E.-J.; Ahrberg, C. D.; Lee, K.-B.; Chung, B. G. Generation of Uniform-Sized Multicellular Tumor Spheroids Using Hydrogel Microwells for Advanced Drug Screening. *Sci. Rep.* **2018**, *8*, 17145.

(10) Lim, J. W.; Shin, K. S.; Moon, J.; Lee, S. K.; Kim, T. A Microfluidic Platform for High-Throughput Screening of Small Mutant Libraries. *Anal. Chem.* **2016**, *88*, 5234−5242.

(11) Ge, Z.; Girguis, P. R.; Buie, C. R. Nanoporous Microscale Microbial Incubators. *Lab Chip* **2016**, *16*, 480−488.

(12) Austin, R. H.; Tung, C.-K.; Lambert, G.; Liao, D.; Gong, X. An Introduction to Micro-Ecology Patches. *Chem. Soc. Rev.* **2010**, *39*, 1049−1059.

(13) Zhang, Q.; Lambert, G.; Liao, D.; Kim, H.; Robin, K.; Tung, C.-K.; Pourmand, N.; Austin, R. H. Acceleration of Emergence of Bacterial Antibiotic Resistance in Connected Microenvironments. *Science* **2011**, *333*, 1764−1767.

(14) Hol, F. J. H.; Galajda, P.; Nagy, K.; Woolthuis, R. G.; Dekker, C.; Keymer, J. E. Spatial Structure Facilitates Cooperation in a Social Dilemma: Empirical Evidence from a Bacterial Community. *PLoS One* **2013**, *8*, No. e77042.

(15) Wilmoth, J. L.; Doak, P. W.; Timm, A.; Halsted, M.; Anderson, J. D.; Ginovart, M.; Prats, C.; Portell, X.; Retterer, S. T.; Fuentes-Cabrera, M. A Microfluidics and Agent-Based Modeling Framework for Investigating Spatial Organization in Bacterial Colonies: The Case of Pseudomonas Aeruginosa and H1-Type VI Secretion Interactions. *Front. Microbiol.* **2018**, *9*, 33.

(16) Li, P.; Dou, X.; Feng, C.; Müller, M.; Chang, M. W.; Frettlöh, M.; Schönherr, H. Isolated Reporter Bacteria in Supramolecular Hydrogel Microwell Arrays. *Langmuir* **2017**, *33*, 7799−7809.

(17) Kou, S.; Cheng, D.; Sun, F.; Hsing, I. M. Microfluidics and Microbial Engineering. *Lab Chip* **2016**, *16*, 432−446.

(18) Levin, I.; Aharoni, A. Evolution in Microfluidic Droplet. *Chem. Biol.* **2012**, *19*, 929−931.

(19) Timm, A. C.; Halsted, M. C.; Wilmoth, J. L.; Retterer, S. T. Assembly and Tracking of Microbial Community Development within a Microwell Array Platform. *J. Visualized Exp.* **2017**, *124*, No. e55701.

(20) Halsted, M.; Wilmoth, J. L.; Briggs, P. A.; Hansen, R. R.; Briggs, D. P.; Timm, A. C.; Retterer, S. T. Development of Transparent Microwell Arrays for Optical Monitoring and Dissection of Microbial Communities. *J. Vac. Sci. Technol., B: Nanotechnol. Microelectron.: Mater., Process., Meas., Phenom.* **2016**, *34*, 06KI03.

(21) Hansen, R. H.; Timm, A. C.; Timm, C. M.; Bible, A. N.; Morrell-Falvey, J. L.; Pelletier, D. A.; Simpson, M. L.; Doktycz, M. J.; Retterer, S. T. Stochastic Assembly of Bacteria in Microwell Arrays Reveals the Importance of Confinement in Community Development. *PLoS One* **2016**, *11*, No. e0155080.

(22) Hooykaas, P. J.J.; Beijersbergen, A. G. M. The Virulence System of Agrobacterium Tumefaciens. *Annu. Rev. Phytopathol.* **1994**, *32*, 157−181.

(23) Barton, I. S.; Fuqua, C.; Platt, T. G. Ecological and Evolutionary Dynamics of a Model Facultative Pathogen: Agrobacterium and Crown Gall Disease of Plants. *Environ. Microbiol.* **2018**, *20*, 16−29.

(24) Peppas, A. N.; Hilt, J. Z.; Khademhosseini, A.; Langer, R. Hydrogels in Biology and Medicine: From Molecular Principles to Bionanotechnology. *Adv. Mater.* **2006**, *18*, 1345−1360.

(25) Tibbitt, M. W.; Kloxin, A. M.; Sawicki, L. A.; Anseth, K. S. Mechanical Properties and Degradation of Chain and Step-Polymerized Photodegradable Hydrogels. *Macromolecules* **2013**, *46*, 2785−2792.

(26) Lutolf, M. P.; Lauer-Fields, J. L.; Schmoekel, H. G.; Metters, A. T.; Weber, F. E.; Fields, G. B.; Hubbell, J. A. Synthetic Matrix Metalloproteinase-Sensitive Hydrogels for the Conduction of Tissue Regeneration: Engineering Cell-Invasion Characteristics. *Proc. Natl. Acad. Sci. U. S. A.* **2003**, *100*, 5413−5418.

(27) Kloxin, A. M.; Kasko, A. M.; Salinas, C. N.; Anseth, K. S. Photodegradable Hydrogels for Dynamic Tuning of Physical and Chemical Properties. *Science* **2009**, *324*, 59−63.

(28) Kloxin, A. M.; Tibbitt, M. W.; Kasko, A. M.; Fairbairn, J. A.; Anseth, K. S. Tunable Hydrogels for External Manipulation of Cellular Microenvironments through Controlled Photodegradation. *Adv. Mater.* **2010**, *22*, 61−66.

(29) Zhu, J. Bioactive Modification of Poly(ethylene glycol) Hydrogels for Tissue Engineering. *Biomaterials* **2010**, *31*, 4639−4656.

(30) Zustiak, S. P.; Leach, J. B. Hydrolytically Degradable Poly(Ethylene Glycol) Hydrogel Scaffolds with Tunable Degradation and Mechanical Properties. *Biomacromolecules* **2010**, *11*, 1348−1357.

(31) Tsukatani, T.; Suenaga, H.; Higuchi, T.; Akao, T.; Ishiyama, M.; Ezoe, K.; Matsumoto, K. Colorimetric Cell Proliferation Assay for Microorganisms in Microtiter Plate Using Water-Soluble Tetrazolium Salts. *J. Microbiol. Methods* **2008**, *75*, 109−116.

DOI: 10.1021/acsabm.8b00592
ACS Appl. Bio Mater. 2019, 2, 266−276

(32) Zustiak, S. P.; Leach, J. B. Characterization of Protein Release from Hydrolytically Degradable Poly(ethylene glycol) Hydrogels. *Biotechnol. Bioeng.* **2011**, *108*, 197−206.
(33) Metters, A.; Hubbell, J. Network Formation and Degradation Behavior of Hydrogels Formed by Michael-Type Addition Reactions. *Biomacromolecules* **2005**, *6*, 290−301.
(34) Tong, X.; Lee, S.; Bararpour, L.; Yang, F. Long-Term Controlled Protein Release from Poly(Ethylene Glycol) Hydrogels by Modulating Mesh Size and Degradation. *Macromol. Biosci.* **2015**, *15*, 1679−1686.
(35) Wong, D. Y.; Ranganath, T.; Kasko, A. M. Low-Dose, Long-Wave UV Light Does Not Affect Gene Expression of Human Mesenchymal Stem Cells. *PLoS One* **2015**, *10*, No. e0139307.
(36) Tibbitt, M. W.; Kloxin, A. M.; Dyamenahalli, K. U.; Anseth, K. S. Controlled Two-Photon Photodegradation of PEG Hydrogels to Study and Manipulate Subcellular Interactions on Soft Materials. *Soft Matter* **2010**, *6*, 5100−5108.
(37) Schneider, C. A.; Rasband, W. S.; Eliceiri, K. W. NIH Image to ImageJ: 25 Years of Image Analysis. *Nat. Methods* **2012**, *9*, 671−675.
(38) Holmes, C. P. Model Studies for New o-Nitrobenzyl Photolabile Linkers: Substituent Effects on the Rates of Photochemical Cleavage. *J. Org. Chem.* **1997**, *62*, 2370−2380.
(39) Qvortrup, K.; Nielsen, T. E. A Photolabile Linker for the Solid-Phase Synthesis of 4-Substituted NH-1,2,3-triazoles. *Chem. Commun.* **2011**, *47*, 3278−3280.
(40) Morton, E. R.; Fuqua, C. Genetic Manipulation of Agrobacterium. *Curr. Protoc. Microbiol.* **2012**, No. Unit 3D.2, DOI: 10.1002/9780471729259.mc03d02s25.
(41) Khan, S. R.; Gaines, J.; Roop, R. M.; Farrand, S. K. Broad-Host-Range Expression Vectors with Tightly Regulated Promoters and Their Use To Examine the Influence of TraR and TraM Expression on Ti Plasmid Quorum Sensing. *Appl. Environ. Microbiol.* **2008**, *74*, 5053.
(42) Fiedler, C. I.; Aisenbrey, E. A.; Wahlquist, J. A.; Heveran, C. M.; Ferguson, V. L.; Bryant, S. J.; McLeod, R. R. Enhanced Mechanical Properties of Photo-Clickable Thiol-Ene PEG Hdrogels Through Repeated Photopolymerization of in-Swollen Macromer. *Soft Matter* **2016**, *12*, 9095−9104.
(43) Adrian, M.; Nijenhuis, W.; Hoogstraaten, R. I.; Willems, J.; Kapitein, L. C. A Phytochrome-Derived Photoswitch for Intracellular Transport. *ACS Synth. Biol.* **2017**, *6*, 1248−1256.
(44) Curtis, S. K.; Cowden, R. R. Demonstration of Sulfhydryl and Disulfide Groups by a Fluorescent Maleimide Procedure. *Histochemistry* **1980**, *68*, 23−28.

DOI: 10.1021/acsabm.8b00592
ACS Appl. Bio Mater. 2019, 2, 266−276